CHAPTER 2

TIME-VARYING FIELDS

This chapter begins with a review of the fundamental laws which govern time-varying electromagnetic fields, including Faraday's law, Maxwell's equations, and boundary conditions at the interface between regions with different electrical properties. The remainder of the chapter is devoted to more practical applications of the theory, including reflection and transmission at a metal surface, diffusion and skin depth, the fields from a short dipole and a small loop, near-field and far-field regions, wave impedance, and power density.

2.1 FARADAY'S LAW

Michael Faraday (1791–1867) was one of the greatest English chemists and physicists. He discovered the principle of electromagnetic induction on August 29, 1831. The electric generator and electric motor are based on Faraday's law. The first evidence for the existence of the electron dates to the work of Faraday. He worked and lectured at the Royal Institution in London for 54 years.

In 1831, Michael Faraday found experimentally that a time-changing magnetic field induced a voltage in a coil immersed in the field, and that the voltage was equal to the time rate of change of the magnetic flux linking the coil. See Fig. 2.1. This form of Faraday's law of induction is expressed as

$$V = -\frac{d\Phi}{dt} \tag{2.1}$$

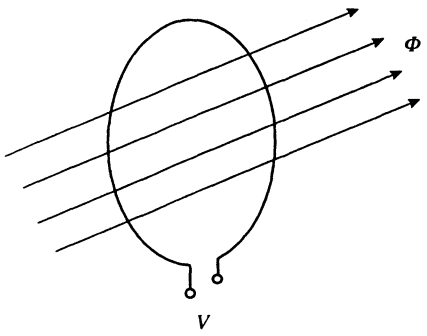

Figure 2.1 Voltage induced in a wire loop by a changing magnetic field (Faraday's law).

where V induced voltage, volts
Φ magnetic flux, webers.

The minus sign in (2.1) follows from Lenz's law which states that the direction of the induced voltage is such that it will tend to produce a current flow that opposes the change of flux.

An important discovery that evolved from Faraday's experiments was that a time-changing magnetic field produces an electric field. This holds in any medium—free space, metals, dielectrics, etc. This is the basis for electromagnetic wave propagation in free space where electric and magnetic fields produce each other in the absence of any sources or a material medium. It is also the basis for one of Maxwell's equations.

Consider any closed path C in space as in Fig. 2.2. Defining the induced voltage V in (2.1) as the line integral of the electric field around C, and using (1.15) to define Φ, results in the following integral form of Faraday's law:

$$\oint_C \mathbf{E} \cdot d\mathbf{l} = -\frac{\partial}{\partial t} \int_S \mathbf{B} \cdot d\mathbf{S}. \tag{2.2}$$

This is also known as the integral form of Maxwell's equation. In a static field, the right-hand side of (2.2) is zero. See (1.6).

A practical application of Faraday's law is the calculation of the voltage induced in an N-turn loop antenna excited by an incident H-field. Refer to Fig. 2.3. In this example, the magnetic field strength H is uniform and normal to the plane of the loop, and has a sinusoidal time variation $\varepsilon^{j\omega t}$. The area of the loop antenna is S. The shape of the loop is of no consequence. It could be square as shown in Fig. 2.3, or circular, triangular, polygonal, etc.

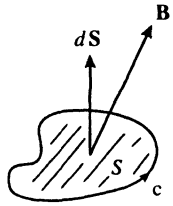

Figure 2.2 Integral form of Faraday's law.

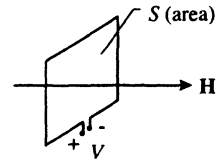

Figure 2.3 Loop antenna.

The received voltage from (2.1) and (2.2) is

$$V = -N\frac{d\Phi}{dt} = -N\frac{d}{dt}\int_S \mathbf{B}\cdot d\mathbf{S}$$

$$V = -\mu_o N S \frac{d}{dt} H\varepsilon^{j\omega t}$$

or

$$V = -j\omega\mu_o N S H\varepsilon^{j\omega t} \quad \text{V.} \tag{2.3}$$

Equation (2.3) is valid for frequencies where the perimeter or circumference of the loop is less than approximately 0.1 wavelength.

2.2 MAXWELL'S EQUATIONS—REGION WITH SOURCES

James Clerk Maxwell (1831–1879), a Scottish scientist, was one of the greatest mathematicians and physicists of the nineteenth century. His best known work, *A Treatise on Electricity and Magnetism* (Oxford University Press, 1873; 3rd edition, 1904) is the foundation of present-day electromagnetic theory. He formulated exact mathematical descriptions of electric and magnetic fields based on Faraday's experiments. In 1864, Maxwell predicted the existence of electromagnetic waves that travel through space at the speed of light. The German physicist Heinrich Hertz proved Maxwell's theories between 1886 and 1888 when he produced electromagnetic waves using an oscillating current generated by the spark of an induction coil.

Consider a region with a charge density ρ and a current density $\mathbf{J}$. This region is characterized by its physical constants of conductivity σ, permeability μ, and permittivity ε, as illustrated in Fig. 2.4.

The presence of an electric field $\mathbf{E}$ in a region with conductivity σ will produce a *conduction current density*

$$\mathbf{J}_{\text{COND}} = \sigma\mathbf{E} \qquad \text{amps/m}^2 \tag{2.4}$$

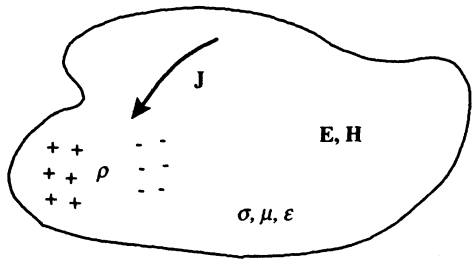

Figure 2.4 Region with sources.

where σ conductivity, mhos/meter
$\mathbf{E}$ electric field strength, V/m.

Equation (2.4) is the field-theoretic form of ohm's law.

In a nonconducting region, a charge density ρ moving with velocity $\mathbf{v}$ is the equivalent of current density. Examples are electron beams in cathode ray tubes and electron streams in ionized gases and plasmas. This equivalent current density is called *convection current density* and is defined as

$$\mathbf{J}_{\text{CONV}} = \rho\mathbf{v} \qquad \text{amps/m}^2 \tag{2.5}$$

where ρ charge density, C/m^3
$\mathbf{v}$ velocity, m/sec.

Total current density $\mathbf{J}$ is the sum of conduction and convection current densities:

$$\mathbf{J} = \mathbf{J}_{\text{COND}} + \mathbf{J}_{\text{CONV}}. \tag{2.6}$$

Current and charge are related by the continuity equation

$$\nabla \cdot \mathbf{J} = -\frac{\partial \rho}{\partial t} \tag{2.7}$$

which states that the net flow of current out of a volume is equal to the negative time rate of change of the volume charge density (or the rate of decrease of charge).

In the formulation of his equations for the electromagnetic field, Maxwell proposed that in a time-varying field, the time rate of change of the electric flux density is equivalent to a current density and produces a magnetic field similar to that produced by a conduction current density (moving charges in conductors) and a convection current density (moving charges in space). This was alluded to in Section 1.3, *Electric Flux*. This

quantity

$$\frac{\partial \mathbf{D}}{\partial t} \qquad \text{amps/m}^2 \tag{2.8}$$

is called *displacement current density.*

The sum of the conduction, convection, and displacement current densities in (2.6) and (2.8) appears in the right-hand side of Maxwell's equation for the curl of the magnetic field.

Maxwell's equations in derivative form for a region with sources $\mathbf{J}$ and ρ (illustrated in Fig. 2.4) are

$$\nabla \times \mathbf{E} = -\frac{\partial \mathbf{B}}{\partial t} \tag{2.9}$$

$$\nabla \cdot \mathbf{D} = \rho \qquad \text{or} \qquad \nabla \cdot \mathbf{E} = \rho/\varepsilon \tag{2.10}$$

$$\nabla \times \mathbf{H} = \mathbf{J} + \frac{\partial \mathbf{D}}{\partial t} \tag{2.11}$$

$$\nabla \cdot \mathbf{B} = 0 \tag{2.12}$$

$$\nabla \cdot \mathbf{J} = -\frac{\partial \rho}{\partial t} \tag{2.13}$$

Equation (2.9) is the differential form of Faraday's law of induction, (2.10) is the differential form of Gauss's law, (2.11) is the differential form of Ampere's law with the displacement current density term added, (2.12) is a consequence of the closed-loop nature of magnetic flux lines (the magnetic field has no divergence), and (2.13) is the continuity equation. (Vector operators in rectangular, cylindrical, and spherical coordinates are reviewed in Appendix E.)

2.3 MAXWELL'S EQUATIONS—SOURCE-FREE REGION

In a source-free region of space, $\sigma = 0$, $\rho = 0$, and therefore $\mathbf{J} = \mathbf{J}_{\text{COND}} + \mathbf{J}_{\text{CONV}} = 0$. Maxwell's equations in a source-free region reduce to the following form:

$$\nabla \times \mathbf{E} = -\mu \frac{\partial \mathbf{H}}{\partial t} \tag{2.14}$$

$$\nabla \cdot \mathbf{D} = \nabla \cdot \mathbf{E} = 0 \tag{2.15}$$

$$\nabla \times \mathbf{H} = \varepsilon \frac{\partial \mathbf{E}}{\partial t} \tag{2.16}$$

$$\nabla \cdot \mathbf{B} = 0. \tag{2.17}$$

If the source-free region is free space, $\varepsilon = \varepsilon_0$ and $\mu = \mu_0$.

2.4 MAXWELL'S EQUATIONS—SINUSOIDAL FIELDS

In most applications, the vector electric and magnetic fields have a sinusoidal time variation and it is advantageous to represent the fields using the complex exponential form $e^{j\omega t}$ (or phasor notation). Thus, $\mathbf{E} = \mathbf{E}_0 e^{j\omega t}$ and $\mathbf{H} = \mathbf{H}_0 e^{j\omega t}$

where $e^{j\omega t} = \cos \omega t + j \sin \omega t$
$\omega = 2\pi f$ radian frequency
f frequency in Hz.

The instantaneous value of the field is given by the imaginary part of $\mathbf{E}_0 e^{j\omega t}$, that is,

$$\mathbf{E}(t) = \mathbf{E}_0 \operatorname{Im} e^{j\omega t} = \mathbf{E}_0 \sin \omega t.$$

When the sinusoidal fields are expressed in complex exponential form, all time derivatives can be replaced by $j\omega$. To illustrate, if $\mathbf{F} = \mathbf{F}_0 e^{j\omega t}$ is a vector field

$$\frac{\partial}{\partial t}\mathbf{F} = \frac{\partial}{\partial t}\mathbf{F}_0 e^{j\omega t} = j\omega \mathbf{F}_0 e^{j\omega t} = j\omega \mathbf{F}.$$

In a region with sources ρ and $\mathbf{J}$ (Fig. 2.4), Maxwell's equations for sinusoidal time-varying fields reduce to

$$\nabla \times \mathbf{E} = -j\omega\mu\mathbf{H} \tag{2.18}$$

$$\nabla \cdot \mathbf{E} = \rho/\varepsilon \tag{2.19}$$

$$\nabla \times \mathbf{H} = \sigma\mathbf{E} + j\omega\varepsilon\mathbf{E} \tag{2.20}$$

$$\nabla \cdot \mathbf{B} = 0 \tag{2.21}$$

$$\nabla \cdot \mathbf{J} = -j\omega\rho. \tag{2.22}$$

In (2.20) it is assumed that the convection current density is zero, i.e., only the conduction current density $\mathbf{J} = \sigma\mathbf{E}$ exists.

In a source-free region of space where $\sigma = 0$, $\rho = 0$, and $\mathbf{J} = 0$, Maxwell's equations for sinusoidal time-varying fields are

$$\nabla \times \mathbf{E} = -j\omega\mu\mathbf{H} \tag{2.23}$$

$$\nabla \cdot \mathbf{E} = 0 \tag{2.24}$$

$$\nabla \times \mathbf{H} = j\omega\varepsilon\mathbf{E} \tag{2.25}$$

$$\nabla \cdot B = 0. \tag{2.26}$$

2.5 BOUNDARY CONDITIONS

In this section, we summarize the boundary conditions on the normal and tangential field components at the interface separating regions with different electrical properties.

Refer to Fig. 2.5, which shows the boundary between two regions with different permittivities ε, permeabilities μ, and conductivities σ. The following relations hold for the tangential components of the fields in the absence of a surface current on the boundary surface:

$$E_1^t = E_2^t \qquad \text{or} \qquad \varepsilon_2 D_1^t = \varepsilon_1 D_2^t \tag{2.27}$$

$$H_1^t = H_2^t \qquad \text{or} \qquad \mu_2 B_1^t = \mu_1 B_2^t \tag{2.28}$$

where the subscripts 1 and 2 refer to regions 1 and 2, and superscript t denotes the tangential field.

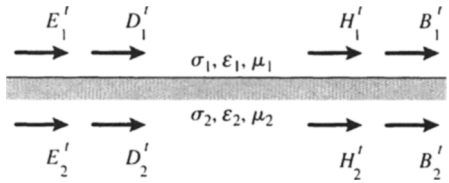

Figure 2.5 Tangential fields at boundary of two regions.

Thus the tangential components of **E** and **H** are continuous across the surface separating two media.

If a surface current J_s exists on the boundary surface, the tangential component of **H** is discontinuous by an amount equal to the surface current:

$$H_1^t - H_2^t = J_s. \tag{2.29}$$

Refer to Fig. 2.6. The following relations hold for the normal components of the fields in the absence of a charge density on the boundary surface:

$$D_1^n = D_2^n \qquad \text{or} \qquad \varepsilon_1 E_1^n = \varepsilon_2 E_2^n \tag{2.30}$$

$$B_1^n = B_2^n \qquad \text{or} \qquad \mu_1 H_1^n = \mu_2 H_2^n. \tag{2.31}$$

Thus the normal components of **D** and **B** are continuous at the boundary between two media.

If a surface charge density ρ_s exists on the boundary surface, the normal component of **D** is discontinuous by an amount equal to the surface charge density:

$$D_1^n - D_2^n = \rho_s. \tag{2.32}$$

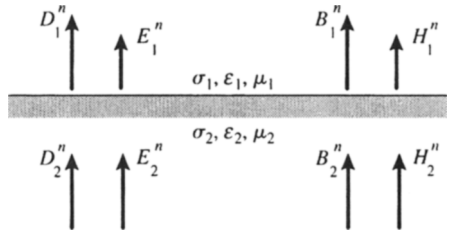

Figure 2.6 Normal field components at boundary of two regions.

The boundary conditions at the surface of a perfect conductor ($\sigma = \infty$) are of special interest. Since the conductivity of metals is so high, in many practical cases they are well approximated by a perfect conductor. An example is a field incident on a metal plane at radio frequencies. This important application will be examined in more detail in the following sections on the reflection and transmission at a conducting slab and on skin depth. Figure 2.7 shows the boundary between a perfect conductor and a dielectric medium. The unit vector normal to the surface is **n**. In a perfect conductor, $E = H = 0$. Also, since the conductor is perfect ($\sigma = \infty$), the skin depth is zero and a true surface current $\mathbf{J}_s$ (in amperes per meter) exists.

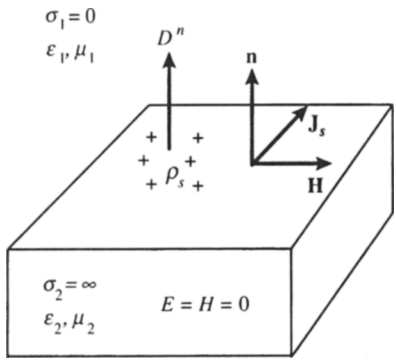

Figure 2.7 Boundary conditions at the surface of a perfect conductor.

Then, from (2.27), (2.29), (2.31) and (2.32), it follows that the fields on the surface of a perfect conductor are

$$E^t = 0 \quad \text{or} \quad \mathbf{n} \times \mathbf{E} = 0 \tag{2.33}$$

$$H^t = J_s \quad \text{or} \quad \mathbf{n} \times \mathbf{H} = \mathbf{J}_s \tag{2.34}$$

$$B^n = 0 \quad \text{or} \quad \mathbf{n} \cdot \mathbf{B} = 0 \tag{2.35}$$

$$D^n = \rho_s \quad \text{or} \quad \mathbf{n} \cdot \mathbf{D} = \rho_s. \tag{2.36}$$

Note that the surface current J_s is equal in magnitude to the tangential magnetic field H^t at the surface, and that the direction of J_s is perpendicular to H^t. This is the basis for the operation and calibration of surface current probes. The typical surface current probe is a calibrated rectangular magnetic loop antenna. When oriented for maximum response, the direction of the surface current is indicated by the transverse dimension of the probe.

2.6 PLANE WAVE INCIDENT ON A CONDUCTING HALF SPACE

Consider a plane wave normally incident on a conducting half space ($z > 0$) as illustrated in Fig. 2.8. Part of the wave is reflected from the surface of the conductor and part of the wave is transmitted into the conductor. (The transmitted wave is also called the *refracted wave.*) This is denoted as follows for the electric field component (the superscripts i, r, and t refer to the incident, reflected, and transmitted waves, respectively):

$$E_x^r = RE_x^i \qquad \text{at the surface } (z = 0) \tag{2.37}$$

$$E_x^t = TE_x^i \qquad \text{at the surface } (z = 0) \tag{2.38}$$

where [2] R reflection coefficient
$T = 1 + R$ transmission coefficient.

The wave impedance of the incident plane wave in air (free space) is

$$Z_o = \frac{E^i}{H^i}. \tag{2.39}$$

The wave impedance of the reflected plane wave in air (traveling in the negative z direction) is [1]

$$-Z_o = \frac{E^r}{H^r}. \tag{2.40}$$

The wave impedance of the plane wave in metal is

$$Z_m = \frac{E^t}{H^t}. \tag{2.41}$$

The reflection and transmission coefficients in terms of the wave impedances are [2]

$$R = \frac{Z_m - Z_0}{Z_m + Z_0} \tag{2.42}$$

$$T = \frac{2\,Z_m}{Z_m + Z_o}. \tag{2.43}$$

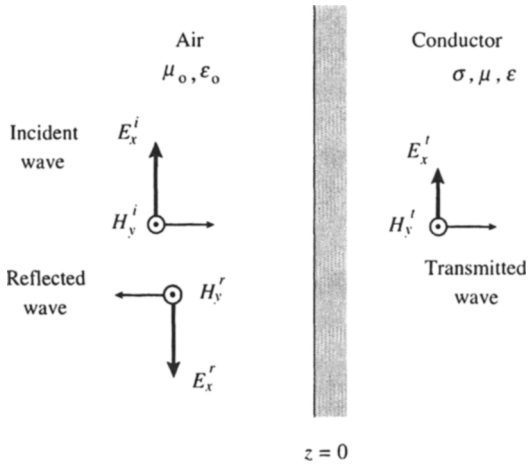

Figure 2.8 Plane wave incident on conducting half space.

Since metal is a much better conductor than air or free space, $Z_m << Z_o$. Then, to a good approximation [1]

$$R \cong -1 \tag{2.44}$$

and

$$T \cong \frac{2Z_m}{Z_o}. \tag{2.45}$$

The reflected and transmitted electric and magnetic fields, from (2.39), (2.40), (2.41), (2.44), and (2.45), are

$$\begin{aligned} E^r &= -E^i \qquad E^t = \frac{2Z_m}{Z_0} E^i \\ H^r &= H^i \qquad H^t = 2H^i. \end{aligned} \tag{2.46}$$

In summary, at the surface of a metal with finite conductivity, to a good approximation, the reflected E field is equal in magnitude and opposite in phase to the incident E field. The transmitted E field is very much smaller than the incident E field (by the ratio $2Z_m/Z_o$). The reflected H field is equal in magnitude and has the same phase as the incident H field. The transmitted H field has twice the magnitude of the incident H field.

An expression for the E field transmission coefficient T in terms of the conductivity and permeability of the metal will now be derived. The intrinsic impedance of free space is

$$Z_o = \sqrt{\frac{\mu_o}{\varepsilon_o}} = 120\pi. \tag{2.47}$$

For a plane wave or TEM wave, the wave impedance is the same as the intrinsic impedance of the medium.

The intrinsic impedance of metal is [1]

$$Z_m = \sqrt{\frac{j\omega\mu}{\sigma}} = (1+j)\sqrt{\frac{\omega\mu}{2\sigma}} \tag{2.48}$$

where $\omega = 2\pi f$ radian frequency, rad/sec
f frequency, Hz.

The magnitude is

$$|Z_m| = \sqrt{\frac{\omega\mu}{\sigma}} = \sqrt{\frac{2\pi f\mu}{\sigma}}. \tag{2.49}$$

Finally, the E-field transmission coefficient in terms of the conductivity and permeability of the metal is found by substituting (2.47) and (2.48) into (2.45):

$$T = (1+j)\sqrt{\frac{f\mu}{3600\pi\sigma}} \tag{2.50}$$

and

$$|T| = \left|\frac{E^t}{E^i}\right| = \sqrt{\frac{f\mu}{1800\pi\sigma}}. \tag{2.51}$$

The relative conductivities and permeabilities of some common metals are listed in Table 2.1. Since there are many different alloys of iron and steel, the values in the table are only typical. The permeabilities of iron and steel are initial permeabilities (i.e., small impressed field). In addition,

Table 2.1 Relative Conductivities and Permeabilities

Metal	σ_r	μ_r
Aluminum	0.61	1
Brass	0.27	1
Iron	0.18	235 (see note)
Copper	1	1
Steel	0.1	180 (see note)

$\sigma = \sigma_r \sigma_c$ where $\sigma_c = 5.8 \times 10^7$mhos/m (conductivity of copper)
$\mu = \mu_r \mu_o$ where $\mu_o = 4\pi \times 10^{-7}$henrys/m (permeability of free space)

Note: At a frequency of approximately 1 kHz

the permeabilities of iron and steel are a function of frequency: the values listed are for a frequency of approximately 1 kHz. Above 1 MHz, the relative permeability of most metals approaches unity.

The E-field transmission coefficient in dB in terms of σ_r and μ_r is

$$T(dB) = 20 \log |T| = -174 + 10 \log \frac{f \mu_r}{\sigma_r}. \tag{2.52}$$

Equation (2.52) is plotted in Fig. 2.9 for copper and steel. The reciprocal of the transmission coefficient (or the negative of the transmission coefficient in dB) is called *reflection loss*.

While the transmitted electric field in metals is orders of magnitude smaller than the incident electric field as evident in Fig. 2.9 (e.g., 114 dB down in copper at 1 MHz), the transmitted magnetic field is twice the magnitude of the incident magnetic field as indicated in (2.46).

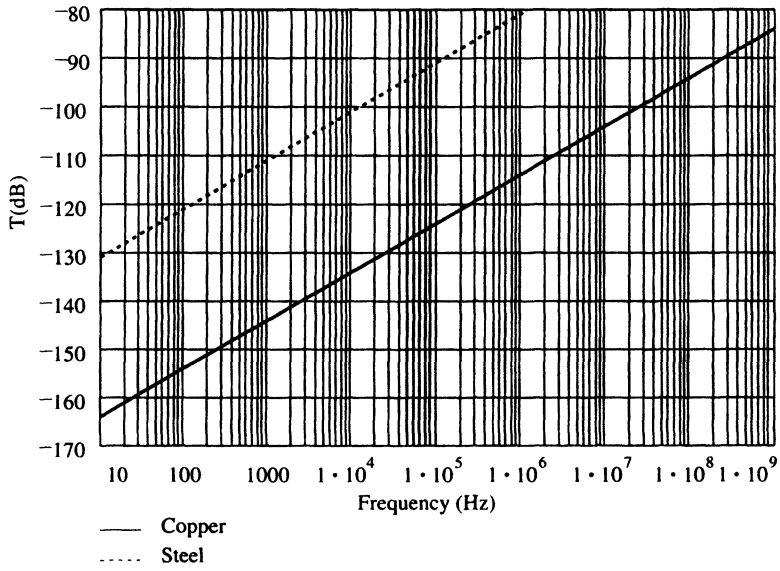

Figure 2.9 E-field transmission coefficient for copper and steel.

2.7 DIFFUSION AND SKIN DEPTH

The transmitted wave in Fig. 2.8 attenuates exponentially in the conductor. The diffusion equation is

$$E_x^t(z) = E_x^t(0)\varepsilon^{-\gamma z} \tag{2.53a}$$

$$H_y^t(z) = H_y^t(0)\varepsilon^{-\gamma z} \tag{2.53b}$$

where $E_x^t(0)$, $H_y^t(0)$ transmitted fields at the surface ($z = 0$)
$\gamma = \alpha + j\beta$ propagation constant
α attenuation constant, nepers/m
β phase constant, rad/m.

The propagation constant γ is

$$\gamma = \sqrt{j\omega\mu\sigma} = \sqrt{\pi f\mu\sigma} + j\sqrt{\pi f\mu\sigma}. \tag{2.54}$$

Then (2.53) can be written as

$$E_x^t(z) = E_x^t(0)\varepsilon^{-\sqrt{\pi f\mu\sigma}z}\varepsilon^{-j\sqrt{\pi f\mu\sigma}z} \tag{2.55a}$$

$$H_y^t(z) = H_y^t(0)\varepsilon^{-\sqrt{\pi f\mu\sigma}z}\varepsilon^{-j\sqrt{\pi f\mu\sigma}z}. \tag{2.55b}$$

Skin depth or *depth of penetration* is defined as the distance the wave must travel in order to decay by an amount equal to $\varepsilon^{-1} = 0.368$, or 8.686 dB. From (2.55), the skin depth δ is

$$\delta = \frac{1}{\sqrt{\pi f\mu\sigma}}. \tag{2.56}$$

In a distance equal to five skin depths, the fields are reduced by a factor of 0.0067, or 43.43 dB. For copper, the skin depth is 8.5 mm at 60 Hz and 0.066 mm at 1 MHz.

From (2.55), the attenuation of the fields as a function of distance is

$$A = \frac{|E_x^t(z)|}{|E_x^t(0)|} = \frac{|H_y^t(z)|}{|H_y^t(0)|} = \varepsilon^{-\sqrt{\pi f\mu\sigma}z} \tag{2.57}$$

where

$$\sqrt{\pi f\mu\sigma} = \text{ attenuation constant in nepers per meter.}$$

The attenuation in dB is

$$A(\text{dB}) = 20\log A = -8.686\sqrt{\pi f\mu\sigma}z \quad \text{dB}. \tag{2.58}$$

The reciprocal of the attenuation (or the negative of the attenuation in dB) is called *absorption loss*.

Expressing (2.58) in terms of the relative permeability and conductivity and the distance z in millimeters, we have

$$A(\text{dB}) = -0.1314z_{mm}\sqrt{f\mu_r\sigma_r} \quad \text{dB}. \tag{2.59}$$

The attenuation in dB per millimeter of distance traveled is

$$A(\text{dB/mm}) = -0.1314\sqrt{f\mu_r\sigma_r} \quad \text{dB/mm}. \tag{2.60}$$

Equation (2.60), which applies to both the electric and magnetic fields, is plotted in Fig. 2.10 for copper and steel. Note that below 1 kHz, the

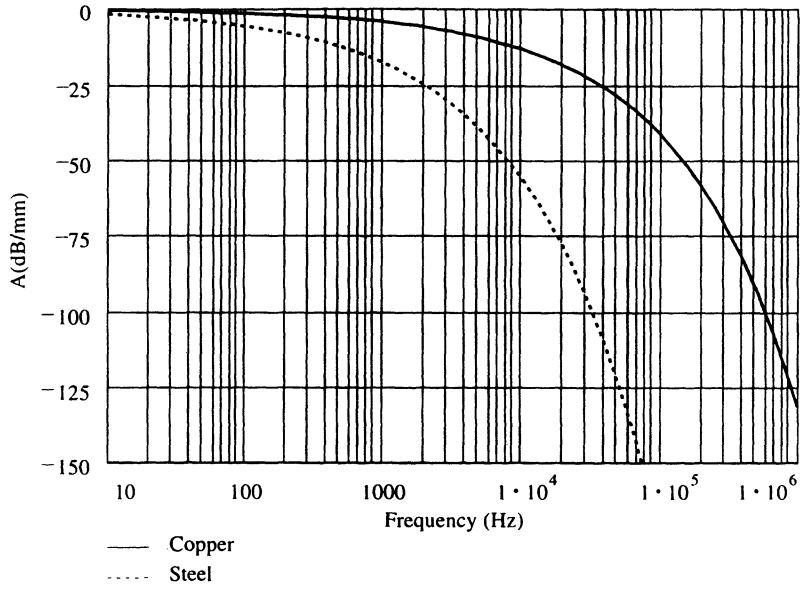

Figure 2.10 Attenuation in dB per mm for copper and steel.

attenuation in copper is less than 4 dB/mm. Above 1 MHz, the attenuation in copper exceeds 130 dB/mm. The attenuation in steel is significantly greater than that in copper.

2.8 TRANSMISSION THROUGH A METAL SHEET (SHIELDING EFFECTIVENESS)

Figure 2.11 shows a plane wave incident on a metal sheet of infinite extent and of thickness τ. We wish to determine how much of the incident wave penetrates the sheet. The shielding factor is defined as

$$\mathcal{S} = \frac{|E_2^t|}{|E^i|}. \tag{2.61}$$

In Section 2.6, the transmitted (refracted) E and H fields at the surface $z = 0$ were derived. In Section 2.7, the attenuation (diffusion) of the E and H fields in the metal as a function of the distance z was derived. The only remaining step to determine the shielding factor $\mathcal{S}$ is to calculate the transmission coefficient at the metal-air boundary at $z = \tau$. The reflected fields at $z = \tau$ and the re-reflected fields at $z = 0$ are neglected because

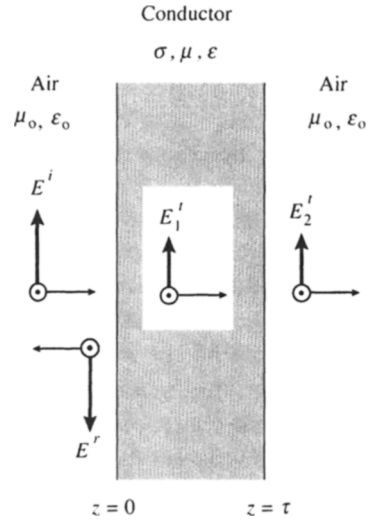

Figure 2.11 Plane wave incident on a metal sheet.

the attenuation in the metal is so high (except at the very low frequencies). See Fig. 2.10.

Let T_2 denote the E-field transmission coefficient at the metal-air boundary at $z = \tau$. By analogy with (2.43)

$$T_2 = \frac{2\,Z_o}{Z_o + Z_m}. \tag{2.62}$$

Since $Z_m << Z_o$, to a good approximation

$$T_2 = 2 \tag{2.63}$$

and

$$T_2(dB) = 20 \log |T_2| = 6 \text{ dB}. \tag{2.64}$$

(This is the opposite of the situation at the air-metal interface at $z = 0$, where the transmitted magnetic field was twice the incident magnetic field.)

The shielding factor is then

$$\mathcal{S} = \frac{|E_2^t|}{|E^i|} = T\,T_2\,A \tag{2.65}$$

or in dB,

$$\mathcal{S}\,(\text{dB}) = T(\text{dB}) + T_2(\text{dB}) + A(\text{dB}). \tag{2.66}$$

Finally, substituting (2.52), (2.64), and (2.59) into (2.66)

$$\mathcal{S}\,(\text{dB}) = -168 + 10\log\frac{f\mu_r}{\sigma_r} - 0.1314\ \tau_{mm}\sqrt{f\mu_r\sigma_r} \tag{2.67}$$

where τ_{mm} thickness of metal sheet, millimeters.

Shielding effectiveness is the reciprocal of the shielding factor $\mathcal{S}$ or, equivalently, the negative of $\mathcal{S}$(dB).

Figures 2.9 and 2.10 can be used to find the shielding factor for copper and steel. First, add +6 dB to the curves in Fig. 2.9 to account for T_2, the transmission coefficient at the surface at $z = \tau$. Next, *multiply* the values in Fig. 2.10 by the thickness of the shield in millimeters. Add the two results. The shielding factor applies to both the electric and magnetic field components of a plane wave. For a copper shield 1 mm thick, the shielding factor is −160 dB at 10 Hz and −240 dB at 1 MHz.

As a practical matter, a thin metal sheet is an effective shield for plane waves, even at very low frequencies. Leakage through apertures is of more importance, especially at higher frequencies. For a more complete discussion of shielding, including near fields, multiple reflections in thin shields, and aperture coupling; see, for instance, Ott [3].

2.9 FIELDS FROM A SHORT DIPOLE

Short dipoles and small loops are the two canonical forms for all electrically small antennas. That is, all electrically small antennas can be represented as a short dipole, small loop, or a combination of these two. See Hansen [4].

The simplest radiator is the short dipole antenna, shown in Fig. 2.12 in spherical coordinates. In many applications, the fields radiated by currents flowing on simple wires and cables can be found by modeling them as a short dipole (or a short monopole). The fields from more complex wire structures can be found by the superposition of the fields of a series-connected array of short dipoles.

The study of the fields from short dipoles and small loops (Section 2.10) also provides insight into the behavior of the fields in the reactive near-field and far-field regions of space surrounding these sources.

The length L of the dipole in Fig. 2.12 is short compared to a wavelength (generally taken to be $L < \lambda/10$, or shorter), and the diameter of the wire is much less than the length.

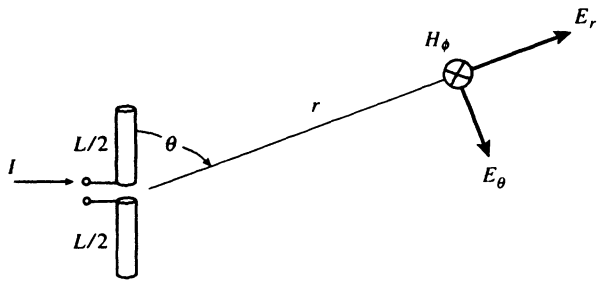

Figure 2.12 Short dipole geometry.

The field quantities in (2.68) to (2.70) are based on the assumption that the current I is uniform (constant) over the length of the dipole. While this current distribution is not physically realizable, it is useful when using series-connected dipoles to approximate actual current distributions on complex wire structures.

In the case of a single short dipole, a triangular current distribution is more representative of the boundary conditions, and thus more accurate. For the triangular distribution, the current at the midpoint is I and the current at the ends of the dipole arms is zero. The fields for the triangular distribution are one-half those for the uniform distribution in (2.68) to (2.70). A thorough discussion of current distributions on wire antennas is given by Balanis [5].

The fields from a short dipole with a uniform current distribution are given below. These equations are from Kraus [6], but in a slightly modified form.

$$E_\theta = 30\, I\, L\, \beta^2 \sin\theta \left[\frac{j}{\beta r} + \frac{1}{(\beta r)^2} - \frac{j}{(\beta r)^3}\right] \varepsilon^{j\omega t} \varepsilon^{-j\beta r} \tag{2.68}$$

$$E_r = 60\, I\, L\, \beta^2 \cos\theta \left[\frac{1}{(\beta r)^2} - \frac{j}{(\beta r)^3}\right] \varepsilon^{j\omega t} \varepsilon^{-j\beta r} \tag{2.69}$$

$$H_\phi = \frac{I\, L\, \beta^2}{4\pi} \sin\theta \left[\frac{j}{\beta r} + \frac{1}{(\beta r)^2}\right] \varepsilon^{j\omega t} \varepsilon^{-j\beta r} \tag{2.70}$$

where E_θ transverse electric field, V/m
H_ϕ transverse magnetic field, A/m
E_r radial electric field, V/m
r distance to field point, m
I current, A

L length of dipole, m
$\beta = \omega/c = 2\pi/\lambda$ phase constant, radians /m
λ wavelength, m
$\omega = 2\pi f$ radians/sec
f frequency, Hz.

Figure 2.13 is a plot, in dB, of E_θ and H_ϕ normalized to $\beta r = 2\pi r/\lambda = 1$, that is,

$$20 \log \frac{E_\theta(\beta r)}{E_\theta(\beta r = 1)} \quad \text{and} \quad 20 \log \frac{H_\phi(\beta r)}{H_\phi(\beta r = 1)}. \tag{2.71}$$

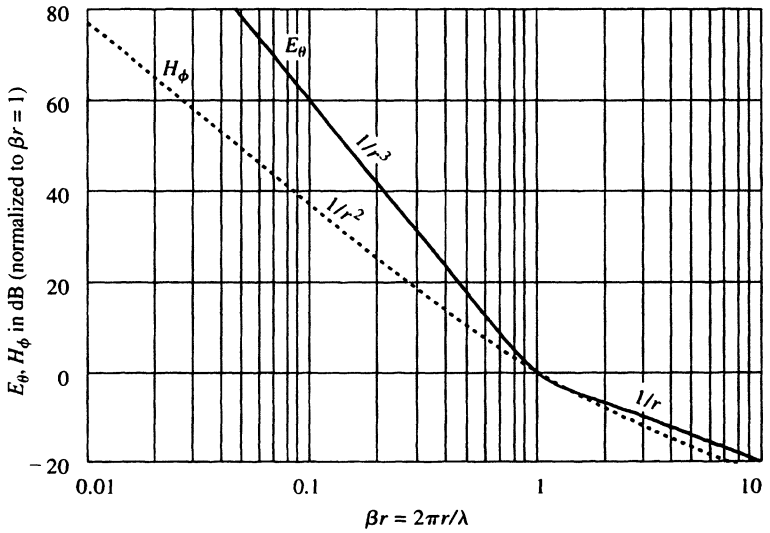

Figure 2.13 Near and far fields of a short dipole.

The transition between the reactive near-field and the far-field regions occurs at a distance of $\beta r = 2\pi r/\lambda = 1$. In the reactive near-field region, E_θ falls off as $1/r^3$ (60 dB per decade distance) and H_ϕ falls off as $1/r^2$ (40 dB per decade distance). In the far-field region, both E_θ and H_ϕ fall off as $1/r$ (20 dB per decade distance) and constitute a propagating plane wave. The radial electric field component E_r, in (2.69), has only $1/r^2$ and $1/r^3$ terms and does not propagate.

In Fig. 2.14, the magnitude of E_θ versus distance r is plotted for three frequencies: 100 kHz, 1 MHz, and 10 MHz. The length of the short dipole is $L = 1$ m, and the current is $I = 1$ ampere. A triangular current distribution is assumed.

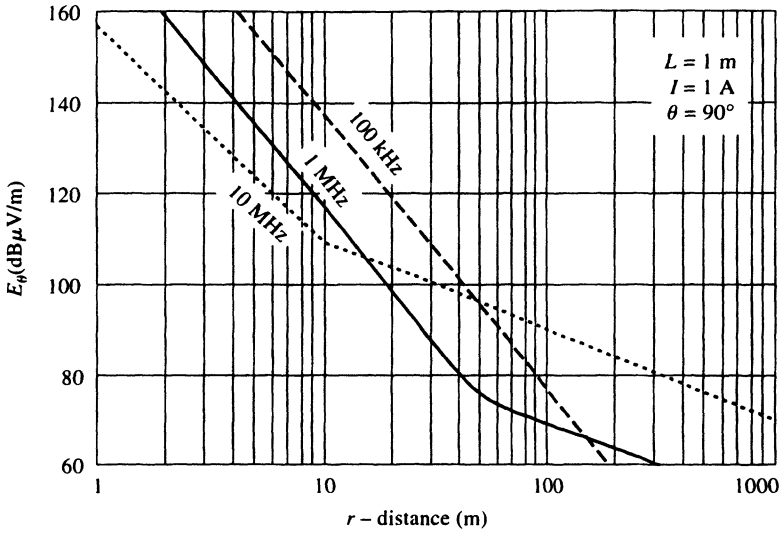

Figure 2.14 Electric field strength versus distance for a short dipole.

Note that in the reactive near-field region, the field strength is greater at the lower frequencies. Conversely, in the far-field region, the field strength increases as the frequency increases.

2.10 FIELDS FROM A SMALL LOOP

Small loops are generally not used as transmitting antennas because they have small radiation resistances compared to short dipoles. However, many unintentional sources of radiation are essentially loop antennas. Examples include transformers, inductors, two-wire transmission lines, and printed circuit boards.

Small loops come in many different shapes, the most common being square and circular. The shape is of no consequence. It is the loop area S that determines the magnitude of the radiated fields.

A small circular loop antenna is shown in Fig. 2.15. The circumference of the loop is small compared to a wavelength and the current I is uniform in amplitude and phase. The fields from a small loop are given below. These equations are a slightly modified form of those due to Schelkunoff and Friis [7].

$$E_\phi = -j\,30\,I\,S\beta^3 \sin\theta \left[\frac{j}{\beta r} + \frac{1}{(\beta r)^2}\right] \varepsilon^{j\omega t} \varepsilon^{-j\beta r} \qquad (2.72)$$

$$H_\theta = \frac{j\,I\,S\beta^3}{4\pi} \sin\theta \left[\frac{j}{\beta r} + \frac{1}{(\beta r)^2} - \frac{j}{(\beta r)^3}\right] \varepsilon^{j\omega t}\varepsilon^{-j\beta r} \tag{2.73}$$

$$H_r = \frac{j\,I\,S\beta^3}{2\pi} \cos\theta \left[\frac{1}{(\beta r)^2} - \frac{j}{(\beta r)^3}\right] \varepsilon^{j\omega t}\varepsilon^{-j\beta r} \tag{2.74}$$

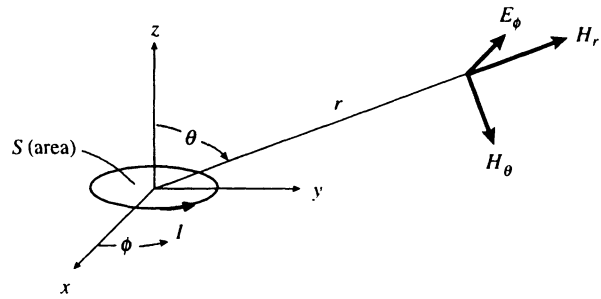

Figure 2.15 Small circular loop geometry.

where E_ϕ transverse electric field, V/m
H_θ transverse magnetic field, A/m
H_r radial magnetic field, A/m
r distance to field point, m
I current, A
S area of loop, m^2
β $= \omega/c = 2\pi/\lambda$ phase constant, rad/m
λ wavelength, m
ω $= 2\pi f$ rad/sec
f frequency, Hz.

In the reactive near-field region ($\beta r < 1$) the transverse magnetic field component H_θ falls off as $1/r^3$ (60 dB per decade distance) and the transverse electric field component E_ϕ falls off as $1/r^2$ (40 dB per decade distance). Compare this with the transverse field components for a short dipole in Fig. 2.13, where the transverse *electric* field falls off as $1/r^3$ and the transverse *magnetic* field falls off as $1/r^2$. The curves in Fig. 2.13 for a short dipole are identical to those for a small loop if E_θ and H_ϕ are replaced by H_θ and E_ϕ, respectively.

As with the short dipole, in the far-field region of a small loop ($\beta r > 1$), both transverse field components E_ϕ and H_θ fall off as $1/r$ (20 dB per decade distance) and constitute a propagating plane wave. The radial

magnetic field component H_r, (2.74), has only $1/r^2$ and $1/r^3$ terms and does not propagate.

Measurements of the rate of attenuation (fall-off) of the transverse field components in the reactive near-field region can be used to determine if a source of radiation is an electric dipole or a magnetic loop. For example, suppose a receiving loop antenna is used to measure the transverse *magnetic* field component at two or more distances from the source, and the data is plotted (preferably in dBμA/m versus distance on a logarithmic scale similar to Fig. 2.13). If the measured fall-off is $1/r^3$ (60 dB per decade distance or 18 dB per octave distance), the source is a magnetic loop. See (2.73). If the fall-off is $1/r^2$ (40 dB per decade distance or 12 dB per octave distance), the source is an electric dipole. See Fig. 2.13 and (2.70).

Conversely, suppose a dipole receiving antenna is used to measure the transverse *electric* field component at two or more distances from the source, and the data is plotted (again, preferably in dBμV/m versus distance on a logarithmic scale similar to Fig. 2.13). If the measured fall-off is $1/r^3$ (60 dB per decade distance or 18 dB per octave distance), the source is an electric dipole. See Fig. 2.13 and (2.68). If the fall-off is $1/r^2$ (40 dB per decade distance or 12 dB per octave distance), the source is magnetic loop. See (2.72).

If the measured fall-off of either the transverse electric or transverse magnetic field component is $1/r$ (20 dB per decade distance or 6 dB per octave distance), then the measurements are in the far-field and it cannot be determined whether the source is an electric dipole or a magnetic loop. It is assumed that the ground-reflected wave is negligible in all of the above.

2.11 NEAR-FIELD AND FAR-FIELD REGIONS

The space surrounding an antenna or other source of radiation is divided into three regions: the reactive near-field region, the radiating near-field region and the far-field region. These are depicted in Fig. 2.16. The characteristics of the fields in these regions are discussed below. See [8] for detailed definitions of these field regions.

In the *reactive near-field* region,

- the reactive fields predominate. These fields fall off as $E \propto 1/r^n$ and $H \propto 1/r^m$ where n, m > 1.
- electromagnetic energy is stored in the fields.

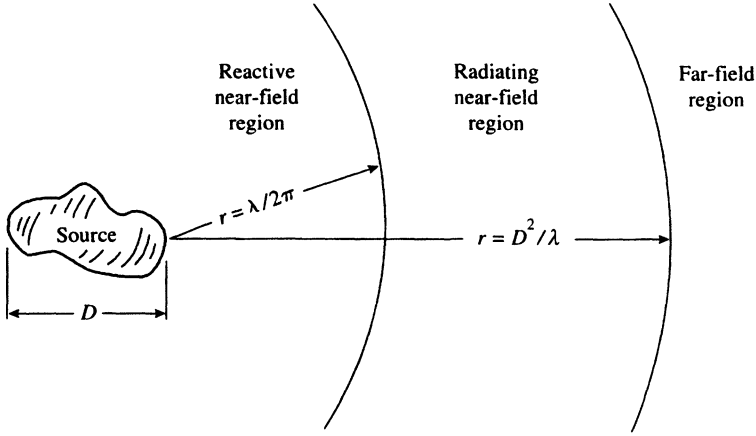

Figure 2.16 Field regions.

- a large radial field component exists.
- the outer boundary of the reactive near-field region is $r = \lambda/2\pi$ where λ is the wavelength.

The *radiating near-field* region has the following characteristics:

- radiation fields predominate
- prediction of the variation of the fields with distance is not possible because the fields oscillate out to a distance equal to $D^2/4\lambda$. See Adams et al. [9].
- this region lies between the reactive near-field region and the far-field region.
- the angular field distribution (the field pattern) depends on the distance.
- this region may not exist if $D << \lambda$ where D is the maximum overall dimension of the source.
- sometimes referred to as the Fresnel region by analogy to optical terminology.

The *far-field* region has the following characteristics:

- the electric and magnetic field components are transverse to the direction of propagation and to each other. That is, they constitute a plane wave.
- the electric and magnetic fields fall off as $1/r$ (inverse distance).

- the angular field distribution (the field pattern) is independent of distance.
- the transition between the radiating near-field region and the far-field region is commonly taken as $r = D^2/\lambda$ (see Hansen [10]) but this distance may vary between $D^2/2\lambda$ and $2D^2/\lambda$ depending on how much deviation from a $1/r$ fall-off can be tolerated in a particular application.
- it is sometimes referred to as the Fraunhofer region by analogy to optical terminology.

Two examples will be used to illustrate the practical application of these concepts. The first example is a microwave oven, shown in Fig. 2.17. The maximum overall dimension of the oven is $D = 0.5$ m, and the oven radiates at a frequency of 2450 MHz. (The source could be any device or antenna having the same size and radiating at the same frequency.) The reactive near-field region only extends out to a distance of $\lambda/2\pi = 2$ cm at this short wavelength. The transition between the radiating near-field region and the far-field region takes place at a distance of $D^2/\lambda = 2.1$ m.

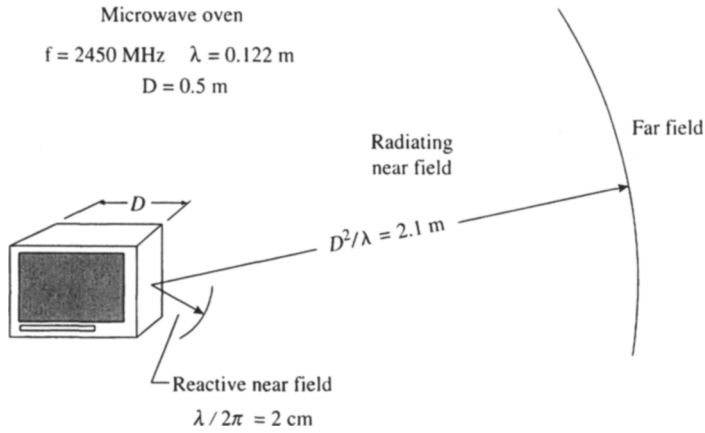

Figure 2.17 Field regions around a microwave oven.

The second example is a personal computer system, shown in Fig. 2.18. The maximum overall dimension of the PC system is the same as that of the microwave oven. The emission from the PC, however, is at a much lower frequency: $f = 1.5$ MHz from the switching power supply. In this example, the reactive near-field region extends out to a distance of 31.8 m. The radiating near-field region does not exist because the dimensions of the source are much smaller than a wavelength ($D^2/\lambda = 1.25$ mm).

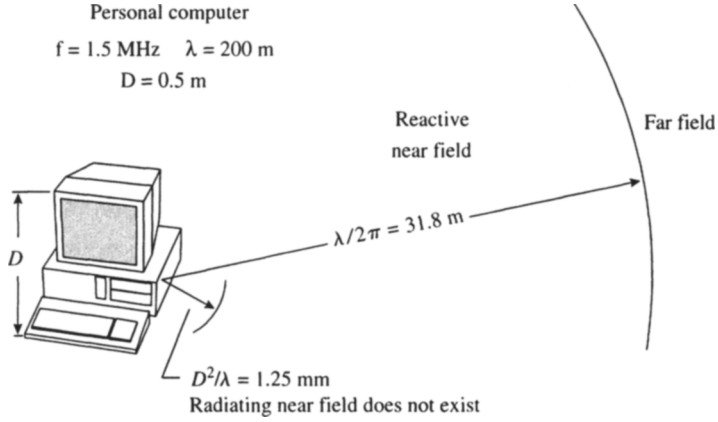

Figure 2.18 Field regions around a personal computer system.

2.12 WAVE IMPEDANCE

The wave impedance of an electromagnetic wave is defined as the ratio of the transverse electric field component to the mutually perpendicular transverse magnetic field component [2]:

$$Z_w = E_t / H_t. \tag{2.75}$$

The modifier transverse means that E_t and H_t lie in a plane that is perpendicular to the direction of propagation, as illustrated in Fig. 2.19.

The definition of wave impedance applies to TEM waves (transverse electromagnetic waves) and to waves having longitudinal components, for example, TE (transverse electric) and TM (transverse magnetic) waves. Included in these categories are waves in free space and other unbounded media, and guided waves on transmission lines and in waveguides.

The wave impedance of a **plane wave or TEM wave** is equal to the intrinsic impedance of the medium in which the wave propagates and is

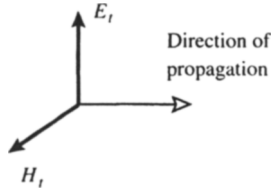

Figure 2.19 Plane wave.

given by

$$Z_w = \sqrt{\frac{\mu}{\varepsilon}} \tag{2.76}$$

where μ and ε are the permeability and permittivity of the medium, respectively.

The wave impedance of a **plane wave in free space** is denoted as Z_o and is equal to

$$Z_o = \sqrt{\frac{\mu_o}{\varepsilon_o}} = 120\pi = 377 \text{ ohms.} \tag{2.77}$$

The wave impedance of the fields from a **short dipole** radiator, from (2.68) and (2.69), is

$$Z_w = \begin{cases} -j\,120\pi(1/\beta r) & \text{near field} \quad (\beta r < 1) \\ 120\pi & \text{far field} \quad (\beta r \geq 1). \end{cases} \tag{2.78}$$

The near-field wave impedance of a short dipole is capacitive and greater than 120 π ohms. The closer to the dipole in terms of wavelength, the higher the wave impedance. For example, at $\beta r = 2\pi r/\lambda = 0.01$, the wave impedance is 37,700 ohms.

Wave impedance, defined as the ratio of the transverse E- and H-field components, conveys no information about the longitudinal field. In the near-field region of a dipole radiator, the radial E field is twice the magnitude of the transverse E field and might be the predominant component in coupling and interference situations.

The wave impedance of the fields from a **small loop** antenna, from (2.72) and (2.73), is

$$Z_w = \begin{cases} j\,120\pi\ \beta r & \text{near field} \quad (\beta r < 1) \\ 120\pi & \text{far field} \quad (\beta r \geq 1). \end{cases} \tag{2.79}$$

The near-field wave impedance of a small loop antenna is inductive and less than 120 π ohms. The closer to the loop in terms of wavelength, the lower the wave impedance. For example, at $\beta r = 2\pi r/\lambda = 0.01$, the wave impedance is 3.77 ohms.

In the near-field region of a loop antenna, the radial H field is twice the magnitude of the transverse H field and might be the predominant component in coupling and interference situations.

2.13 POWER DENSITY AND HAZARDOUS RADIATION

Human exposure to high-level electromagnetic fields can cause harmful effects. Recommended levels of maximum permissible exposure (MPE) to radio frequency electromagnetic fields are given in IEEE C95.1-1991 [11]. The MPEs are given in terms of the rms electric (E) and magnetic (H) field strengths, and in terms of the equivalent free-space plane-wave average power density S_{AV}. The relationships between field strengths and power density in the reactive near-field and far-field regions are reviewed below.

The instantaneous magnitude and direction of power flow per unit area (power density) in an electromagnetic field are given by the instantaneous Poynting vector $\mathbf{S}$:

$$\mathbf{S} = \mathbf{E} \times \mathbf{H} \qquad \text{watts/m}^2. \tag{2.80}$$

For a sinusoidal time varying field, the average Poynting vector is

$$\mathbf{S}_{AV} = \frac{1}{2} \operatorname{Re} \mathbf{E} \times \mathbf{H}^* = \operatorname{Re} \mathbf{E}_{\text{rms}} \times \mathbf{H}^*_{\text{rms}} \tag{2.81}$$

where $\mathbf{H}^*$ denotes the complex conjugate of $\mathbf{H}$ and where the *rms* values of $\mathbf{E}$ and $\mathbf{H}$ are equal to the peak values divided by $\sqrt{2}$.

Figure 2.20 illustrates the electric and magnetic fields as space vectors and as phasors in the time domain. The space angle between the field vectors is α, and the phase angle between E and H is θ.

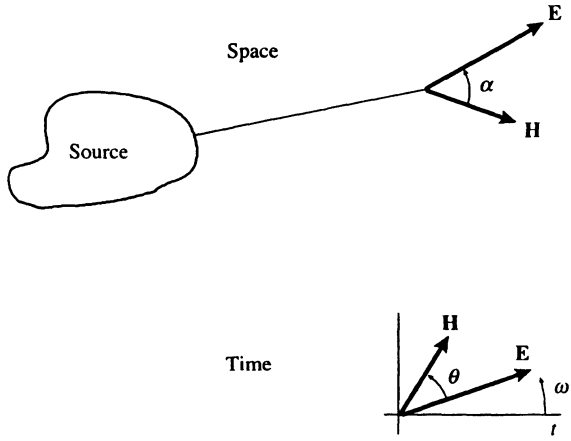

Figure 2.20 Space and time-domain representation of E and H fields.

At a single frequency, the magnitude of the average power density is

$$S_{AV} = E_{\text{rms}} H_{\text{rms}} \sin\alpha \cos\theta \qquad \text{W/m}^2. \tag{2.82}$$

Equation (2.82) is general and applies to both reactive near fields and plane waves.

There is no commercial instrument which can measure the true average power-density expressed in (2.82) in the reactive near-field region. Commercial radiation hazard meters are calibrated in units of *equivalent* free-space plane-wave average power density, but use probes which measure either the electric field component or the magnetic field component. Typical E-field probes use two or three orthogonal dipoles. Typical H-field probes use three orthogonal loops.

Care should be taken when interpreting readings taken with radiation hazard meters in the reactive near field. In high-impedance fields, measurements with H-field probes will read lower than the true power density, in some cases by orders of magnitude, depending on the wave impedance. Conversely, in low-impedance fields, measurements with E-field probes will read lower than the true power density. This is the reason that the maximum permissible exposures in IEEE C95.1 are stated in terms of the rms electric (E) and magnetic (H) field strengths, and in terms of the *equivalent* free-space plane-wave average power density S_{AV}.

For a plane wave in free space with sinusoidal time variation,

$$E = 120\pi\ H$$
$$\sin\alpha = 1$$
$$\cos\theta = 1$$

and (2.82) can be expressed as

$$S_{AV} = \frac{E_{\text{rms}}^2}{3770} \qquad \text{mW/cm}^2 \tag{2.83}$$

or

$$S_{AV} = 37.7\ H_{\text{rms}}^2 \qquad \text{mW/cm}^2 \tag{2.84}$$

or

$$S_{AV} = \frac{E_{\text{rms}} H_{\text{rms}}}{10} \qquad \text{mW/cm}^2 \tag{2.85}$$

where E is in V/m, H is in A/m, and S_{AV} is in milliwatts per square centimeter.

The maximum permissible exposures for an uncontrolled environment from IEEE C95.1-1991 are shown in Table 2.2. E, H, and power density as a function of frequency are plotted in Fig. 2.21.

Table 2.2 Maximum Permissible Exposure for Uncontrolled Environments

Frequency Range (MHz)	*E* (V/m)	*H* (A/m)	Power Density (mW/cm^2)
0.003–0.1	614	163	
0.1–1.34	614	$16.3/f$	
1.34–3.0	$823.8/f$	$16.3/f$	
3.0–30	$823.8/f$	$16.3/f$	
30–100	27.5	$158.3/f^{1.668}$	
100–300	27.5	0.0729	0.2
300–3000			$f/1500$
3000–15,000			$f/1500$
15,000–300,000			10.0

Note: f = frequency in MHz.
Source:

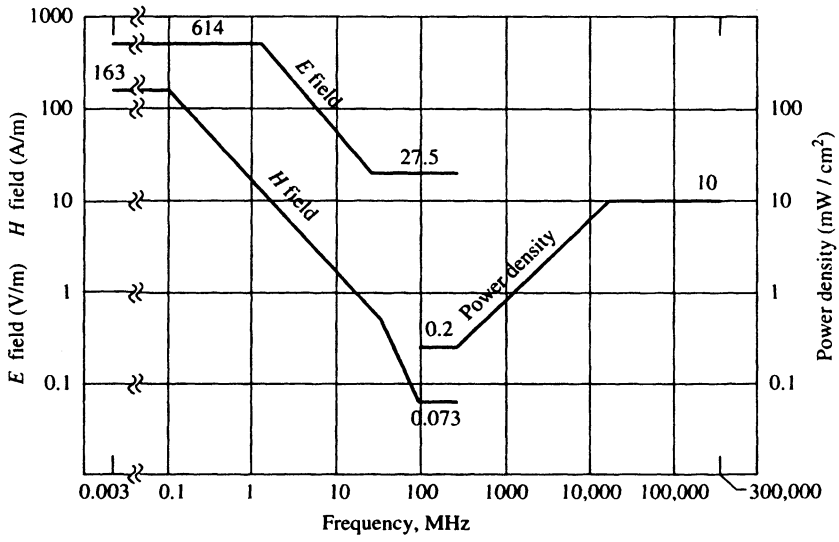

Figure 2.21 Maximum permissible exposure for an uncontrolled environment. (IEEE C95.1-1991). *Copyright ©1992, IEEE. All rights reserved.*

References

[1] J. D. Kraus and K. R. Carver, *Electromagnetics*, second edition, McGraw-Hill, New York, 1973.

[2] R. E. Collin, *Field Theory of Guided Waves*, second edition, IEEE Press, New York, 1991.

[3] H. W. Ott, *Noise Reduction Techniques in Electronic Systems*, John Wiley & Sons, New York, 1976.

[4] R. C. Hansen, *Reference Data for Radio Engineers*, Chapter 32 - Antennas, Howard W. Sams & Co., Division of MacMillan, Inc., Indianapolis, Indiana, seventh edition, 1989.

[5] C. A. Balanis, *Antenna Theory: Analysis and Design*, Harper and Row, Publishers, Inc., New York, 1982.

[6] J. D. Kraus, *Antennas*, McGraw-Hill, New York, 1950.

[7] S. A. Schelkunoff and H. T. Friis, *Antennas: Theory and Practice*, John Wiley & Sons, New York, 1952.

[8] IEEE Std 100-1977, *IEEE Standard Dictionary of Electrical and Electronics Terms*, published by IEEE, New York, distributed in cooperation with Wiley-Interscience, New York, 1977.

[9] A. T. Adams, Y. Leviatan and K. S. Nordby, "Electromagnetic Near Fields as a Function of Electrical Size," *IEEE Transactions on Electromagnetic Compatibility*, vol. EMC-25, no. 4, pp. 428–432, November 1983.

[10] R. C. Hansen and L. L. Bailin, "A New Method of Near Field Analysis," *IRE Transactions on Antennas and Propagation*, pp. S458–S467, December 1959.

[11] IEEE C95.1-1991, *IEEE Standard for Safety Levels with Respect to Human Exposure to Radio Frequency Electromagnetic Fields, 3 kHz to 300 GHz*, Institute of Electrical and Electronic Engineers, 1992. Recognized as an American National Standard (ANSI).